IEEE Access
Multidisciplinary ⋮ Rapid Review ⋮ Open Access Journal

Received 23 June 2023, accepted 2 July 2023, date of publication 4 July 2023, date of current version 10 July 2023.

Digital Object Identifier 10.1109/ACCESS.2023.3292303

RESEARCH ARTICLE

A Metasurface-Based MIMO Antenna With Compact, Wideband, and High Isolation Characteristics for Sub-6 GHz 5G Applications

HUY-HUNG TRAN[1,2], TUNG THE-LAM NGUYEN[3], HOAI-NAM TA[4], AND DUY-PHONG PHAM[5]

[1]Faculty of Electrical and Electronic Engineering, Phenikaa University, Hanoi 12116, Vietnam
[2]Phenikaa Research and Technology Institute (PRATI), Hanoi 11313, Vietnam
[3]IT Department, FPT University, Greenwich Vietnam, Hanoi 11312, Vietnam
[4]Faculty of Radio Electronics Engineering, Le Quy Don Technical University, Hanoi 10000, Vietnam
[5]Faculty of Electronics and Telecommunications, Electric Power University, Hanoi 10000, Vietnam

Corresponding author: Huy-Hung Tran (hung.tranhuy@phenikaa-uni.edu.vn)

ABSTRACT A compact metasurface (MS) based MIMO antenna with wideband operation and high isolation characteristics is proposed for sub-6 GHz applications. A single element is constructed by a slot coupled with 2×2 unit cells MS. For mutual coupling suppression, the MS of each MIMO element is grounded at proper positions by metallic vias. Compared to other reported designs, the proposed antenna possesses several unique features including a simple decoupling method with no extra space requirement, compact size, and wideband operation. For verification, the measurements have been implemented on a fabricated prototype with overall dimensions of $0.85\lambda_c \times 0.48\lambda_c \times 0.03\lambda_c$ (λ_c is the free-space wavelength at center operating frequency) and the center-to-center element spacing of $0.43\lambda_c$. The measured results indicate that the proposed design has a wide operating bandwidth of 15% (3.7 − 4.3 GHz) with high isolation of better than 25 dB. In addition, the measured maximum gain is about 4.1 dBi, and good diversity performance is also achieved. The proposed MIMO antenna is a potential candidate for 5G applications operating at the NR77 band.

INDEX TERMS Compact, high isolation, metasurface, MIMO, shorting vias, wideband.

I. INTRODUCTION

Achieving optimal isolation in a compact size is one of the most critical challenges in designing a multiple-input-multiple-output (MIMO) antenna. Additionally, modern wireless communication systems require high-speed data transfer or multiple services working on the same device, leading to strong demand for wideband antennas. Therefore, the literature on achieving high isolation and wideband operation in a compact size is notably rich, with numerous proposed techniques.

For mutual coupling suppression, a lot of attempts have been made in the literature. Among them, the simplest method is to cut the ground plane with various shapes of slots [1], [2], [3]. However, this technique might not be particularly appealing when the antenna is mounted on a metallic object. Using parasitic elements [4], [5], [6], [7], [8], [9], [10], [11] or metamaterial [12], [13], [14], [15], [16], [17], [18], [19] without disturbing the ground plane, which is introduced in between or close to the radiating elements, is another solution to decouple antennas. Although high isolation can be achieved, these methods always require extra space in either a horizontal or a vertical direction and significantly increases the design complexity as well. To overcome these deficiencies, simple decoupling methods utilizing strip

The associate editor coordinating the review of this manuscript and approving it for publication was Tutku Karacolak.

lines printed on the upper surface of the dielectric resonator antenna (DRA) [20] or metallic vias [21] placed inside the DRA have been reported. The main advantage of [20] and [21] is that no extra space for decoupling structure is needed, which shows potential for the simple and compact MIMO antenna system.

In terms of operating BW, slot/monopole structures [22], [23], [24], [25] are well-known for wideband operation. However, these antenna types feature an omnidirectional beam with low gain radiation. This paper only concentrates on the MIMO antenna having a unidirectional radiation pattern and higher gain than the slot/monopole antennas. It is worth noting that most of the reported directional MIMO designs focus on narrowband operation with high isolation. The literature review indicates that wideband operation with a unidirectional broadside beam can be easily obtained with DR antennas [15], [16], [21] and patch antennas [9], [10]. To conclude, most of these designs have limited operating BW, which is typically less than 15%. They also suffer from disadvantages such as large size, high profile, or complicated decoupling networks.

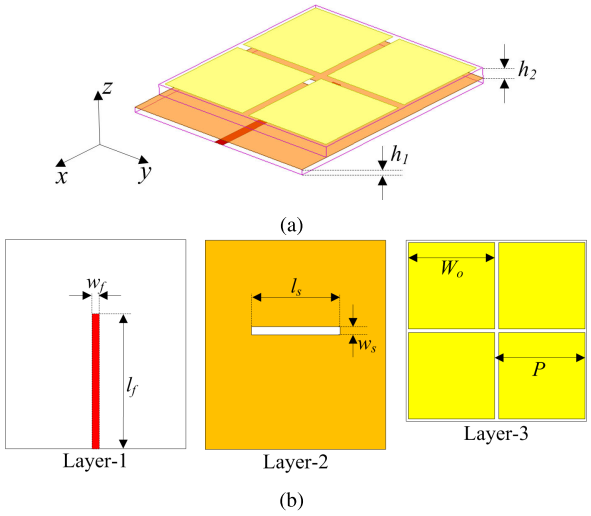

FIGURE 1. Geometry of the single element. (a) Overview and (b) Top-view of each layer.

In this paper, a metasurface (MS) based MIMO antenna with compact size, wideband, and high isolation characteristics is presented. The MIMO element is constructed by a slot coupled with 2 × 2 unit cells MS. It is worth noting that the use of shorting vias as the decoupling network has been applied in the DRA [21], but this antenna only has a narrowband operation. In [19], extra space between the MIMO elements is required for the shorting vias. In contrast, for the presented work, the shorting vias are positioned inside the MIMO elements. Thus, it doesn't require any extra space, which contributes to simplifying the design's architecture and miniaturizing the antenna's dimensions. Meanwhile, the proposed antenna still achieves wideband operation and high isolation. This distinguishes the proposed work from the MIMO antennas using similar decoupling methods.

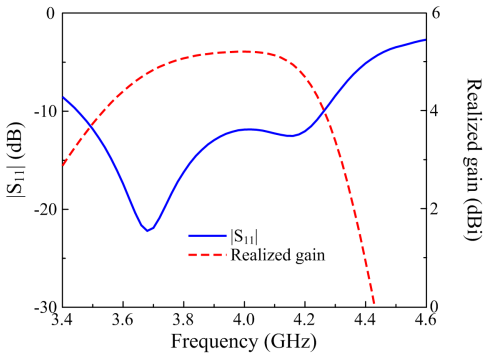

FIGURE 2. Performance of the single element.

II. ANTENNA DESIGN

A. SINGLE ELEMENT

The MS antenna has been extensively investigated as a new kind of antenna with a low profile and wideband characteristics [26], [27]. In this design, the proposed antenna is constructed by an array of 2 × 2 unit cells with dimensions of $W_0 \times W_0$ and periodicity of P, as presented in Fig. 1. The dielectric substrate FR-4 with a relative dielectric constant of 4.4 and a loss tangent of 0.02 is used throughout and the thicknesses are 0.8 and 1.6 mm for the bottom and top layers, respectively. A slot is located at the center of the ground plane and the proposed antenna is excited through a 50-Ω microstrip line. The antenna is modeled and characterized using a commercial simulation tool High-Frequency Structure Simulator (HFSS). The optimized dimensions of the single element are as follows: $h_1 = 0.8$, $h_2 = 1.6$, $l_f = 24.1$, $w_f = 1.5$, $l_s = 16$, $w_s = 1.5$, $W_0 = 15$, $P = 16$ (unit: mm).

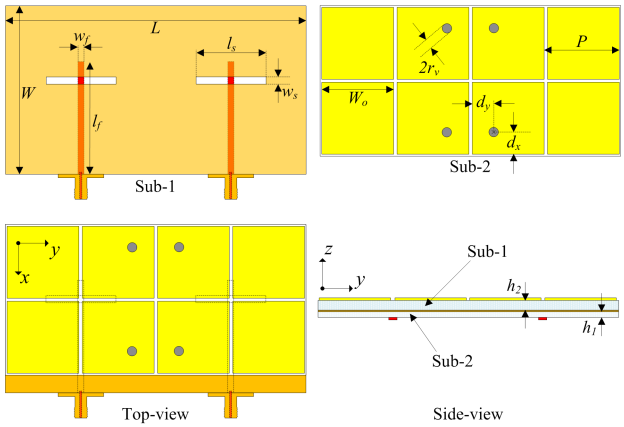

FIGURE 3. Geometry of the proposed 2-element MIMO antenna.

Fig. 2 presents the simulated $|S_{11}|$ and broadside gain of the proposed MS antenna. As observed, the design with a compact size of $0.47\lambda_c \times 0.41\lambda_c \times 0.03\lambda_c$ exhibits wide −10 dB impedance BW of 21.1%, ranging from

3.44 to 4.25 GHz. Here, the principle for wideband performance is to produce two nearby resonances. The lower band is generated from the slot and the higher band is produced by the MS. The slot's length is chosen about half-effective wavelength at the desired frequency, while the MS is initially predicted by using characteristic mode analysis to define the operating band [28], [29]. In terms of gain, the gain values within the impedance BW are better than 3.5 dBi and the maximum gain is 5.2 dBi. Note that with the help of the MS, the gain is about 3 dB higher than the slotted antenna due to the increase in the radiating aperture. Besides, the electromagnetic fields are confined between the ground plane and the MS layer. Thus, it contributes to decreasing the backward radiation. In the meantime, the front-to-back ratio is enhanced. In fact, when more unit cells are utilized, the antenna's gain can be further improved and the backward radiation can be further mitigated. However, this results in a large footprint antenna, which is not our target in this paper.

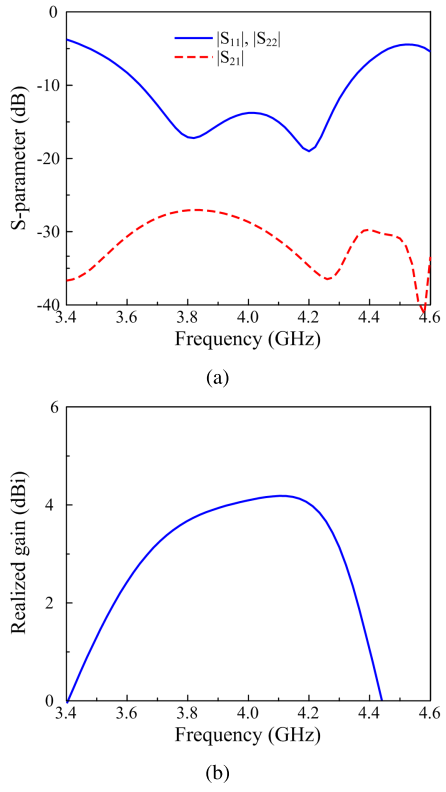

FIGURE 4. Performance of the 2-element MIMO antenna. (a) S-parameter and (b) realized gain.

B. TWO-ELEMENT MIMO ANTENNA

Based on the proposed MS antenna element, its MIMO system is further investigated. The proposed MIMO design is presented in Fig. 3. The MIMO antenna consists of two identical elements arranged in the H-plane configuration. Note that the distance between the MIMO elements is chosen so that the periodicity of the unit cells remains unchanged. Due to the close proximity, the isolation between the MIMO elements is quite low at about 15 dB. For mutual coupling reduction, four vias are employed to connect the MS unit cells to the ground plane. The positions of the vias are as shown in Fig. 3. The optimized dimensions of the proposed 2-element MIMO antenna are $L = 64$, $W = 36$, $h_1 = 0.8$, $h_2 = 1.6$, $l_f = 24$, $w_f = 1.1$, $l_s = 14.8$, $w_s = 1.5$, $W_0 = 15.2$, $P = 16$, $r_v = 1$, $d_x = 3.6$, $d_y = 5$ (unit: mm).

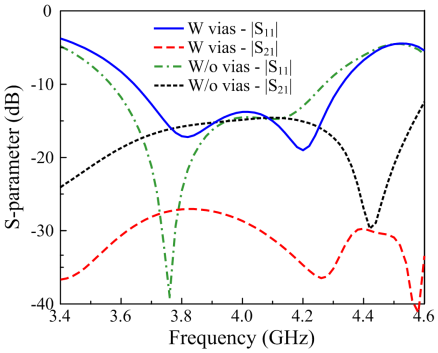

FIGURE 5. Simulated S-parameter of the MIMO antenna with and without vias.

The simulated S-parameter in terms of reflection coefficient and transmission coefficient and realized gain of the proposed 2-element MIMO antenna are depicted in Fig. 4. As observed, the antenna has a wideband operation with −10 dB impedance BW from 3.64 to 4.32 GHz, equivalent to about 17.1%. Meanwhile, the simulated isolation values are always better than 27 dB across the impedance BW. In terms of gain, Fig. 4(b) shows the broadside gain when the antenna is excited at Port-1. The data indicate that the gain across the −10 dB impedance BW ranges from 3.0 to 4.2 dBi.

III. DECOUPLING MECHANISM

For a better understanding of the role of shorting vias, the performances of the MIMO antenna with and without shorting vias are considered. Fig. 5 shows the simulated reflection coefficient $|S_{11}|$ and transmission coefficient $|S_{21}|$ of these antennas. In both cases, the antenna shows good impedance matching in the frequency range from 3.6 to 4.4 GHz. In terms of isolation, the coupled MIMO antenna has an isolation of about 14 dB. With the presence of four shorting vias, the isolation is significantly enhanced to 27 dB.

To explain the decoupling mechanism, the simulated surface current distributions on the ground plane, shorting vias, as well as MS of the antennas with and without decoupling networks are given in Fig. 6. Note that the simulated results are attained with Port-1 excitation. For the coupled MIMO, Fig. 6(a) observes a strong coupling from the excited element to the non-excited element in both the MS layer and ground plane layer. Here, the current highly concentrates around the slot and two unit cells close to the excited element. For the MIMO with the proposed decoupling network, the current is just strongly distributed on the excited element. Meanwhile, the coupling is blocked by the shorting vias with strong

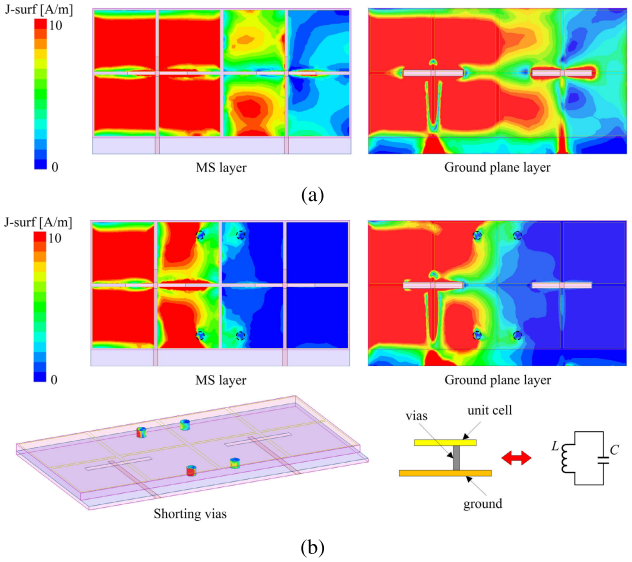

FIGURE 6. Simulated current distributions at 4.0 GHz on (a) Coupled MIMO without decoupling network, and (b) decoupled MIMO with the proposed decoupling network.

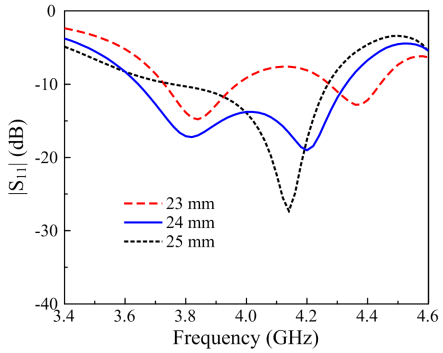

FIGURE 7. Simulated $|S_{11}|$ of the proposed MIMO antenna for different lengths of l_f.

currents concentrated on the vias, as shown in Fig. 6(b). In fact, the presence of vias contributes to generating LC circuits, which can provide a rejected frequency band [30]. Here, C denotes the capacitance between the unit cell and the ground. L is the inductance of the shorting vias.

IV. ANTENNA OPTIMIZATION

In this section, antenna optimization is presented. The process is divided into three main steps: impedance matching, wideband operation, and isolation. All design parameters are considered for each step. Nonetheless, only the key parameters are chosen to present for brevity. It is noted that when one parameter is studied, the others are kept at optimal values as presented in Section II-B.

A. IMPEDANCE MATCHING OPTIMIZATION

The antenna's impedance matching can be controlled by tuning the length of the feeding lines, l_f. Fig. 7 shows the $|S_{11}|$ against the variations of l_f. As observed, this parameter

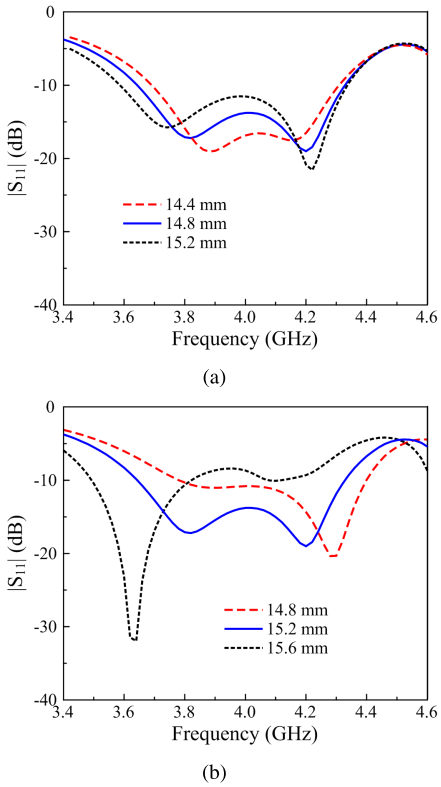

FIGURE 8. Simulated $|S_{11}|$ of the proposed MIMO antenna against the variations of (a) l_s and (b) W_0.

strongly affects the matching performance of the proposed MIMO antenna. With $l_f = 24$ mm, the antenna shows the best -10 dB impedance BW. A shorter or longer feeding line significantly degrades the matching performance.

B. WIDEBAND OPERATION OPTIMIZATION

The wideband operation is obtained by combining the resonances from the slot and the MS. Fig. 8 shows the $|S_{11}|$ with different values of the slot's length, l_s, and the unit cell dimension, W_0. As shown in Fig. 8(a), changing l_s only has a significant effect on the lower band operation. Longer slot results in lower $|S_{11}|$ resonance. Meanwhile, the higher resonance remains unchanged with the variation of l_s. Similarly, the higher band operation can be controlled by tuning the unit cell dimension, W_0. As presented in Fig. 8(b), larger W_0 leads to lower resonance in the high-frequency band. Since the MS acts as an effective radiating aperture of the proposed antenna, W_0 also causes a strong impact on the lower operating band, which shifts upwards as W_0 decreases.

C. ISOLATION OPTIMIZATION

As shown in Section III, the mutual coupling between the MIMO elements is suppressed with the help of the shorting vias. According to Fig. 6(b), the vias has a significant effect on the field distributions. Therefore, their position and size are critical parameters in determining the isolation of the proposed MIMO antenna. Fig. 9 shows the antenna

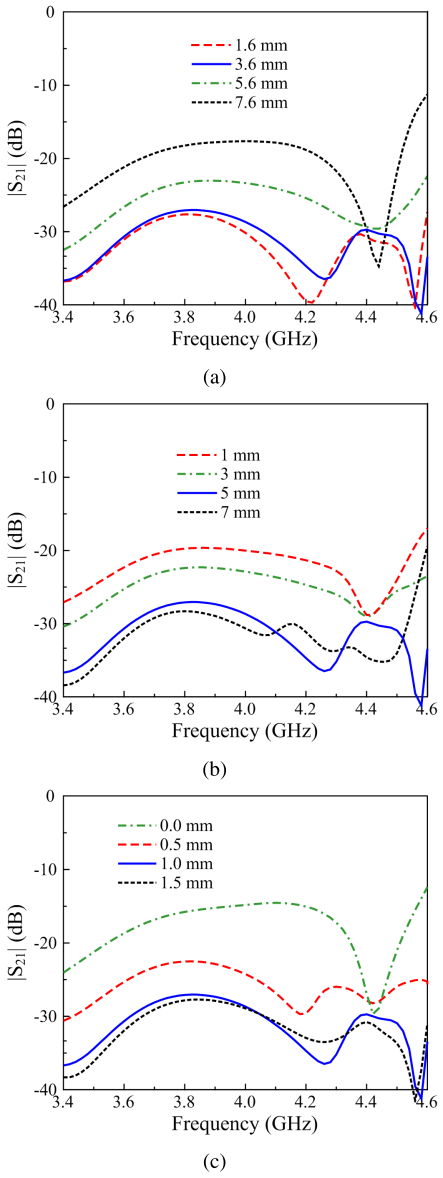

FIGURE 9. Simulated $|S_{21}|$ of the proposed antenna against the variations of (a) d_x, (b) d_y and (c) r_v.

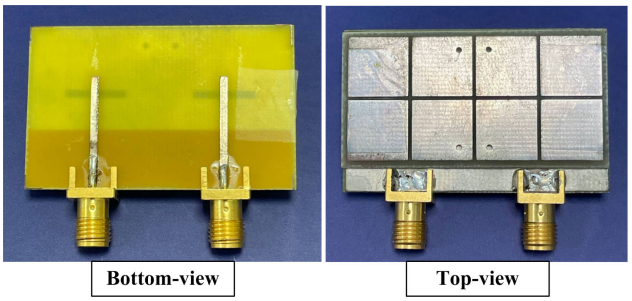

FIGURE 10. Photographs of the fabricated MIMO antenna prototype.

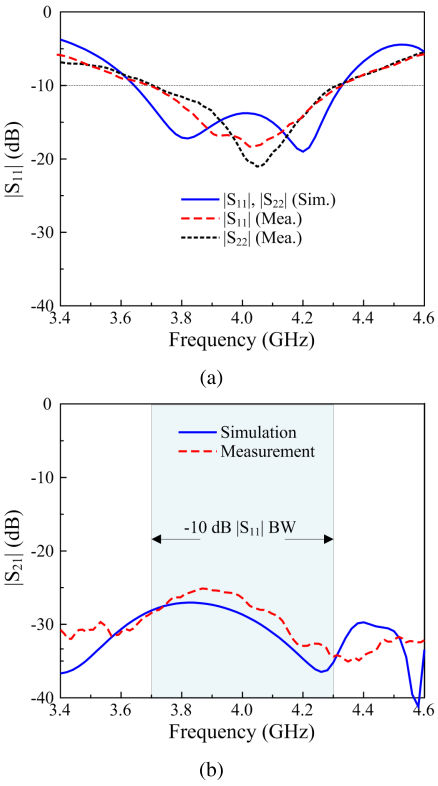

FIGURE 11. Simulated and measured S-parameter of the proposed MIMO antenna. (a) $|S_{11}|$, (b) $|S_{21}|$.

transmission coefficients for different values of d_x, d_y, and r_v. The simulated data indicates that the isolation performance is significantly affected by d_x and d_y. Besides, r_v is also another important parameter in mutual coupling reduction. Better isolation can be achieved with the increase of r_v. Note that the effect of these parameters on the $|S_{11}|$ performance is insignificant. Although $d_x = 7.6$ mm, $d_y = 1.6$ mm, and $r_v = 1.5$ mm show better isolation, the $|S_{11}|$ results are slightly degraded. Thus, these parameters are chosen so that both impedance matching and isolation over the operating band are the best.

V. MEASUREMENT RESULTS

To confirm the proposed concept, measurements have been implemented on a fabricated prototype. Photographs of the fabricated antenna with respect to the bottom- and top-view are shown in Fig. 10. Fig. 11 presents the simulated and measured S-parameter of the proposed MIMO antenna. The simulations are well-matched with the measurements with only a small discrepancy in the −10 dB impedance BW, which could be attributed to the imperfection in experimental setup and fabrication tolerances. With reference to Fig. 11(a), a wide −10 dB impedance BW of 15% (3.7 - 4.3 GHz) is achieved. Along with this, the measured isolation provided in Fig. 11(b) is more than 25 dB.

Due to the geometrical symmetry, only the far-field results for Port 1 excitation are shown. Fig. 12 shows the simulated and measured gain of the proposed design. The measured gain values within the operating band are in the

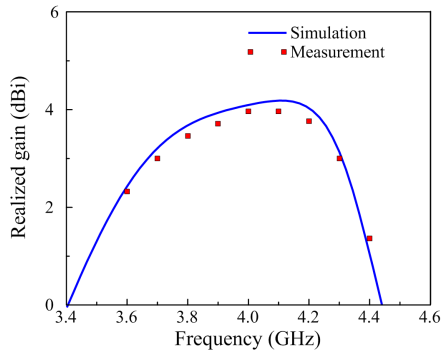

FIGURE 12. Simulated and measured broadside gain of the proposed MIMO antenna.

range of 3.0 to 4.1 dBi. The 3-D and 2-D gain radiation patterns at different frequencies of 3.8 and 4.2 GHz are plotted in Figs. 13 and 14. It observes a similar behavior between the simulation and measurement results. The antenna also shows good broadside radiation pattern.

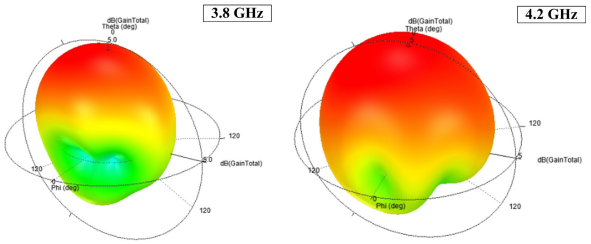

FIGURE 13. Simulated 3-D radiation patterns at different frequencies.

VI. MIMO DIVERSITY PERFORMANCE

The diversity performance of the proposed antenna is evaluated through several parameters including Envelope Correlation Coefficient (ECC), Diversity Gain (DG), Channel Capacity Loss (CCL), and Mean Effective Gain (MEG). The calculated equations of these parameters are presented in [31] and [32] and thus, they are not shown here.

The ECC indicates the correlation between the adjacent MIMO antenna elements. In a practical environment, the acceptable value of ECC must be less than 0.5. The DG demonstrates the reliability and quality of a MIMO antenna in wireless systems, and it must be high at about 10 dB in the operating frequency band. In terms of transmission, the CCL indicates the information that can be transmitted with almost zero loss in the communication channel. The predefined CCL value is smaller than 0.4 bits/s/Hz. With respect to MEG, it is defined as the ratio of power received by the MIMO antenna to the power received by the isotropic antenna. The acceptable MEG is less than 3 dB. The calculated ECC, DG, CCL, and MEG parameters are shown in Fig. 15. In the operating frequency band from 3.7 to 4.3 GHz, all the MIMO parameters satisfy the predefined values for practical applications.

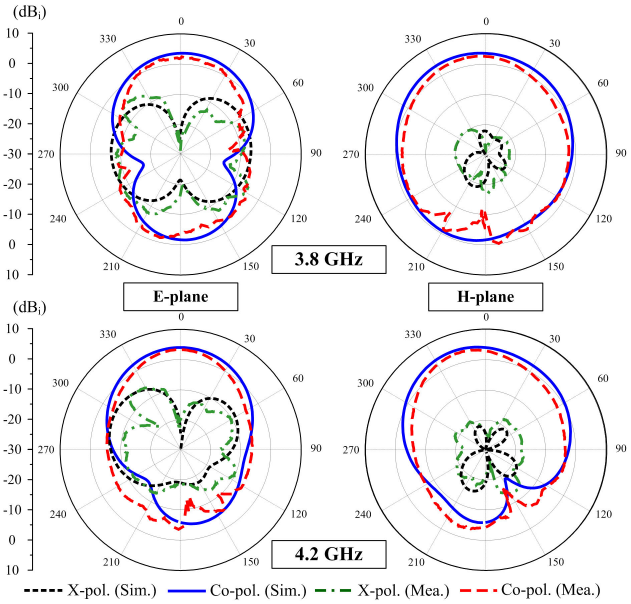

FIGURE 14. Simulated and measured radiation patterns of the proposed MIMO antenna.

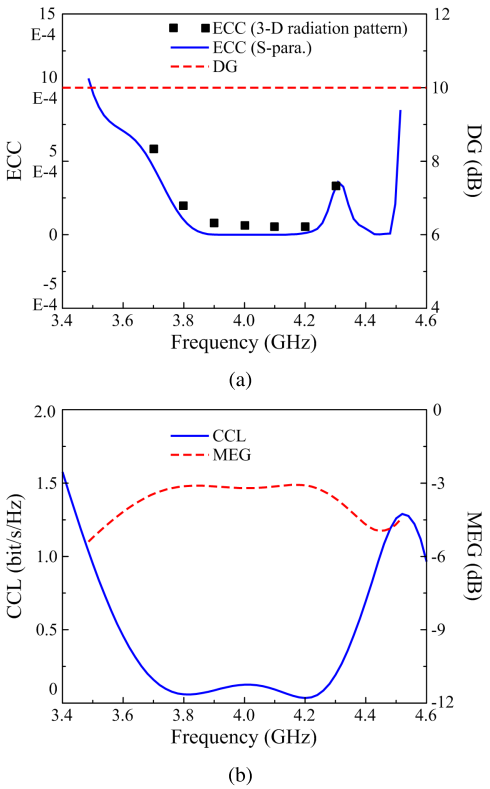

FIGURE 15. Calculated diversity parameters of the proposed MIMO antenna. (a) ECC, DG, and (b) CCL, MEG.

VII. PERFORMANCE COMPARISON

To demonstrate the advantages of the proposed design, Table 1 shows a comparison among the wideband MIMO designs in the literature. In general, the attractive features

TABLE 1. Comparison among wideband MIMO antennas.

Ref.	No. of ports	Overall size (λ_c)	Extra space*	Spacing (λ_c)	BW (%)	Iso. (dB)
[4]	2	$1.44 \times 0.90 \times 0.06$	Yes	0.58	14.8	≥ 20
[9]	4	N/G	Yes	0.50	19.6	≥ 17
[10]	4	$1.51 \times 1.51 \times 0.04$	Yes	0.76	15.5	≥ 20
[12]	2	$1.30 \times 0.87 \times 0.15$	Yes	0.36	7.7	≥ 20
[15]	2	$2.82 \times 2.82 \times 0.40$	Yes	0.50	14.8	≥ 20
[16]	2	$1.52 \times 1.52 \times 0.38$	Yes	0.50	10.0	≥ 26
[19]	4	$1.74 \times 1.74 \times 0.04$	Yes	0.91	15.9	≥ 32
[21]	2	$1.90 \times 0.96 \times 0.13$	No	0.50	7.3	≥ 30
Prop.	2	$0.85 \times 0.48 \times 0.03$	No	0.43	15.0	≥ 25

*: Extra space for decoupling structures

of our design are compact size, small element spacing, wide BW, as well as acceptable isolation. Especially, no extra space is required for the decoupling network. On the other hand, most of the reported works require additional space, which leads to a large lateral size. In comparison with the proposed antenna, there are several noticeable issues. Although the MIMO designs in [9], [10], and [19] have wider BW, they have smaller isolation and/or larger element spacing. Additionally, better isolation can be achieved in [16] and [21]. However, significant high profile and large lateral dimensions are critical drawbacks of such designs. In [12], this work has smaller element spacing, but with limited operating BW and isolation.

VIII. CONCLUSION

A 2-element MIMO antenna with the capability of offering wideband operation, high isolation, as well as compact size features has been presented and investigated in this paper. The MIMO elements are arranged in the H-plane configuration and the metallic shorting vias are employed for mutual coupling reduction. Four vias connect the unit cells to the ground plane, and therefore, no extra space is required. The final design has a compact overall size of $0.85\lambda_c \times 0.48\lambda_c \times 0.03\lambda_c$ and a center-to-center element spacing of $0.43\lambda_c$. The experiment results prove that the proposed antenna exhibits a wide impedance BW of 15% (3.7 - 4.3 GHz) and the isolation is higher than 25 dB. Additionally, the proposed antenna achieves good MIMO diversity performance with all diversity parameters satisfying the predefined values for practical applications. According to the achieved performance, the proposed MIMO antenna is very promising for compact sub-6 GHz 5G applications.

REFERENCES

[1] Q. Li, A. P. Feresidis, M. Mavridou, and P. S. Hall, "Miniaturized double-layer EBG structures for broadband mutual coupling reduction between UWB monopoles," *IEEE Trans. Antennas Propag.*, vol. 63, no. 3, pp. 1168–1171, Mar. 2015.

[2] K. Wei, J.-Y. Li, L. Wang, Z.-J. Xing, and R. Xu, "Mutual coupling reduction by novel fractal defected ground structure bandgap filter," *IEEE Trans. Antennas Propag.*, vol. 64, no. 10, pp. 4328–4335, Oct. 2016.

[3] C. Chiu, F. Xu, S. Shen, and R. D. Murch, "Mutual coupling reduction of rotationally symmetric multiport antennas," *IEEE Trans. Antennas Propag.*, vol. 66, no. 10, pp. 5013–5021, Oct. 2018.

[4] H. H. Tran and N. Nguyen-Trong, "Performance enhancement of MIMO patch antenna using parasitic elements," *IEEE Access*, vol. 9, pp. 30011–30016, 2021.

[5] H. Qi, X. Yin, L. Liu, Y. Rong, and H. Qian, "Improving isolation between closely spaced patch antennas using interdigital lines," *IEEE Antennas Wireless Propag. Lett.*, vol. 15, pp. 286–289, 2016.

[6] T. Pei, L. Zhu, J. Wang, and W. Wu, "A low-profile decoupling structure for mutual coupling suppression in MIMO patch antenna," *IEEE Trans. Antennas Propag.*, vol. 69, no. 10, pp. 6145–6153, Oct. 2021.

[7] K.-L. Wu, C. Wei, X. Mei, and Z.-Y. Zhang, "Array-antenna decoupling surface," *IEEE Trans. Antennas Propag.*, vol. 65, no. 12, pp. 6728–6738, Dec. 2017.

[8] M. Li, B. G. Zhong, and S. W. Cheung, "Isolation enhancement for MIMO patch antennas using near-field resonators as coupling-mode transducers," *IEEE Trans. Antennas Propag.*, vol. 67, no. 2, pp. 755–764, Feb. 2019.

[9] S. Maddio, G. Pelosi, M. Righini, S. Selleri, and I. Vecchi, "Mutual coupling reduction in multilayer patch antennas via meander line parasites," *Electron. Lett.*, vol. 54, no. 15, pp. 922–924, Jul. 2018.

[10] K. D. Xu, J. Zhu, S. Liao, and Q. Xue, "Wideband patch antenna using multiple parasitic patches and its array application with mutual coupling reduction," *IEEE Access*, vol. 6, pp. 42497–42506, 2018.

[11] M. Li, M. Y. Jamal, L. Jiang, and K. L. Yeung, "Isolation enhancement for MIMO patch antennas sharing a common thick substrate: Using a dielectric block to control space-wave coupling to cancel surface-wave coupling," *IEEE Trans. Antennas Propag.*, vol. 69, no. 4, pp. 1853–1863, Apr. 2021.

[12] X. Zou, G. Wang, Y. Wang, and B. Zong, "Metasurface-based coupling suppression for wideband multiple-input-multiple-output antenna arrays," *Opt. Exp.*, vol. 29, no. 25, p. 41643, Nov. 2021.

[13] Z. Qamar, U. Naeem, S. A. Khan, M. Chongcheawchamnan, and M. F. Shafique, "Mutual coupling reduction for high-performance densely packed patch antenna arrays on finite substrate," *IEEE Trans. Antennas Propag.*, vol. 64, no. 5, pp. 1653–1660, May 2016.

[14] M.-C. Tang, Z. Chen, H. Wang, M. Li, B. Luo, J. Wang, Z. Shi, and R. W. Ziolkowski, "Mutual coupling reduction using meta-structures for wideband, dual-polarized, and high-density patch arrays," *IEEE Trans. Antennas Propag.*, vol. 65, no. 8, pp. 3986–3998, Aug. 2017.

[15] M. Farahani, J. Pourahmadazar, M. Akbari, M. Nedil, A. R. Sebak, and T. A. Denidni, "Mutual coupling reduction in millimeter-wave MIMO antenna array using a metamaterial polarization-rotator wall," *IEEE Antennas Wireless Propag. Lett.*, vol. 16, pp. 2324–2327, 2017.

[16] R. Karimian, A. Kesavan, M. Nedil, and T. A. Denidni, "Low-mutual-coupling 60-GHz MIMO antenna system with frequency selective surface wall," *IEEE Antennas Wireless Propag. Lett.*, vol. 16, pp. 373–376, 2017.

[17] Z. Wang, L. Zhao, Y. Cai, S. Zheng, and Y. Yin, "A meta-surface antenna array decoupling (MAAD) method for mutual coupling reduction in a MIMO antenna system," *Sci. Rep.*, vol. 8, no. 1, p. 3152, Feb. 2018.

[18] F. Liu, J. Guo, L. Zhao, X. Shen, and Y. Yin, "A meta-surface decoupling method for two linear polarized antenna array in sub-6 GHz base station applications," *IEEE Access*, vol. 7, pp. 2759–2768, 2019.

[19] M. A. Sufian, N. Hussain, H. Askari, S. G. Park, K. S. Shin, and N. Kim, "Isolation enhancement of a metasurface-based MIMO antenna using slots and shorting pins," *IEEE Access*, vol. 9, pp. 73533–73543, 2021.

[20] Y. Zhang, J.-Y. Deng, M.-J. Li, D. Sun, and L.-X. Guo, "A MIMO dielectric resonator antenna with improved isolation for 5G mm-wave applications," *IEEE Antennas Wireless Propag. Lett.*, vol. 18, no. 4, pp. 747–751, Apr. 2019.

[21] Y. M. Pan, X. Qin, Y. X. Sun, and S. Y. Zheng, "A simple decoupling method for 5G millimeter-wave MIMO dielectric resonator antennas," *IEEE Trans. Antennas Propag.*, vol. 67, no. 4, pp. 2224–2234, Apr. 2019.

[22] J. Park, M. Rahman, and H. N. Chen, "Isolation enhancement of wide-band MIMO array antennas utilizing resistive loading," *IEEE Access*, vol. 7, pp. 81020–81026, 2019.

[23] L. Wang, Z. Du, H. Yang, R. Ma, Y. Zhao, X. Cui, and X. Xi, "Compact UWB MIMO antenna with high isolation using fence-type decoupling structure," *IEEE Antennas Wireless Propag. Lett.*, vol. 18, no. 8, pp. 1641–1645, Aug. 2019.

[24] Y.-Y. Liu and Z.-H. Tu, "Compact differential band-notched stepped-slot UWB-MIMO antenna with common-mode suppression," *IEEE Antennas Wireless Propag. Lett.*, vol. 16, pp. 593–596, 2017.

[25] S. Zhang and G. F. Pedersen, "Mutual coupling reduction for UWB MIMO antennas with a wideband neutralization line," *IEEE Antennas Wireless Propag. Lett.*, vol. 15, pp. 166–169, 2016.

[26] F. Costa, O. Luukkonen, C. R. Simovski, A. Monorchio, S. A. Tretyakov, and P. M. de Maagt, "TE surface wave resonances on high-impedance surface based antennas: Analysis and modeling," *IEEE Trans. Antennas Propag.*, vol. 59, no. 10, pp. 3588–3596, Oct. 2011.

[27] H. H. Tran and T. T. Le, "A metasurface based low-profile reconfigurable antenna with pattern diversity," *AEU, Int. J. Electron. Commun.*, vol. 115, Feb. 2020, Art. no. 153037.

[28] H. H. Tran, C. D. Bui, N. Nguyen-Trong, and T. K. Nguyen, "A wideband non-uniform metasurface-based circularly polarized reconfigurable antenna," *IEEE Access*, vol. 9, pp. 42325–42332, 2021.

[29] F. H. Lin and Z. N. Chen, "Low-profile wideband metasurface antennas using characteristic mode analysis," *IEEE Trans. Antennas Propag.*, vol. 65, no. 4, pp. 1706–1713, Apr. 2017.

[30] C.-L. Wang, G.-H. Shiue, W.-D. Guo, and R.-B. Wu, "A systematic design to suppress wideband ground bounce noise in high-speed circuits by electromagnetic-bandgap-enhanced split powers," *IEEE Trans. Microw. Theory Techn.*, vol. 54, no. 12, pp. 4209–4217, Dec. 2006.

[31] A. Kumar, A. Q. Ansari, B. K. Kanaujia, J. Kishor, and L. Matekovits, "A review on different techniques of mutual coupling reduction between elements of any MIMO antenna. Part 1: DGSs and parasitic structures," *Radio Sci.*, vol. 56, no. 3, pp. 1–25, Mar. 2021.

[32] K. L. Chung, L. Chen, G. Lai, K. Zheng, Z. Wang, H. Cui, and B. Feng, "Three-element circularly polarized MIMO antenna with self-decoupled probing method for B5G-V2X communications," *Alexandria Eng. J.*, vol. 70, pp. 553–567, May 2023.

HUY-HUNG TRAN received the B.S. degree in electronics and telecommunications from the Hanoi University of Science and Technology, Hanoi, Vietnam, in 2013, the M.S. degree in electrical engineering from Ajou University, in 2015, and the Ph.D. degree in electrical engineering from Dongguk University, South Korea, in 2020. He is currently a Lecturer with the Department of Electrical and Electronic Engineering, Phenikaa University, Hanoi. His research interests include circularly polarized antennas, MIMO antennas, metamaterial-based antennas, and reconfigurable antennas.

TUNG THE-LAM NGUYEN received the B.E. degree in electronics and telecommunications from the Hanoi University of Science and Technology, Hanoi, Vietnam, in 2009, and the M.E. and Ph.D. degrees in electronics and electrical engineering from Dongguk University, Seoul, South Korea, in 2013 and 2016, respectively. He was a Senior Engineer with the Radar Center, Viettel High Technology Industries Corporation, Viettel Group, Hanoi, from 2016 to 2022. He is currently a Lecturer with the Computing Department, Greenwich Vietnam, FPT University, Hanoi. His research interests include RF and millimeter-wave devices, semiconductor device modeling, and deep learning.

HOAI-NAM TA received the B.E. degree in electronics and telecommunications and the M.E. degree in electronics and electrical engineering from Le Quy Don Technical University, Hanoi, Vietnam, in 2016 and 2022, respectively. He is currently a Researcher with the Center for Telecommunication Engineering, Faculty of Radio Electronics Engineering, Le Quy Don Technical University. His research interests include millimeter-wave devices, antenna designs, non-contact sensors, and FPGA-based system designs.

DUY-PHONG PHAM received the B.E. degree in telecommunications engineering from the University of Communications and Transport, Hanoi, Vietnam, in 2000, the master's degree in electronics and telecommunications from the Hanoi University of Technology, Hanoi, in 2007, and the Ph.D. degree in telecommunications engineering from the Vietnam Research Institute of Electronics, Informatics, and Automation, Hanoi, in 2013. He was a Researcher with the Posts and Telecommunications Institute of Technology, from 2000 to 2005. He is currently the Dean of the Faculty of Electronics and Telecommunications, Electric Power University, Hanoi. His main research interests include radio propagation, antenna design for radio communications, underwater acoustic communication, electromagnetic interference on telecommunication systems due to power systems, and lightning protection for telecommunication systems.